Mineralogy and Petrology
https://doi.org/10.1007/s00710-023-00825-2

RESEARCH

Three new copper-lead selenite bromides obtained by chemical vapor transport: $Pb_5Cu^+_4(SeO_3)_4Br_6$, $Pb_8Cu^{2+}(SeO_3)_4Br_{10}$, and the synthetic analogue of the mineral sarrabusite, $Pb_5Cu^{2+}(SeO_3)_4(Br,Cl)_4$

Oleg I. Siidra[1,2] · Vasili Yu. Grishaev[1] · Evgeni V. Nazarchuk[1] · Roman A. Kayukov[1]

Received: 12 December 2022 / Accepted: 5 April 2023

Abstract
Three new copper-lead selenite bromides were synthesized by chemical vapor transport reactions. $Pb_5Cu^+_4(SeO_3)_4Br_6$ is monoclinic, space group *C*2/*m*, *a* = 17.7248(14), *b* = 5.5484(5), *c* = 12.7010(10) Å, β = 103.398(2)º, *V* = 1215.08(17) Å^3, R_1 = 0.024; $Pb_8Cu^{2+}(SeO_3)_4Br_{10}$ is orthorhombic, space group *I*222, *a* = 9.5893(5), *b* = 12.4484(9), *c* = 12.7927(6) Å, *V* = 1527.08(15) Å^3, R_1 = 0.027; $Pb_5Cu^{2+}(SeO_3)_4(Br,Cl)_4$ is monoclinic, *C*2/*c*, *a* = 24.590(6) Å, *b* = 5.5786(14) Å, *c* = 14.248(4) Å, β = 102.883(7)º, *V* = 1905.3(9) Å^3, R_1 = 0.026. The crystal structure of $Pb_5Cu^+_4(SeO_3)_4Br_6$ consists of two distinct parts: corner- and edge-sharing Cu^+Br_4 tetrahedra form infinite $[Cu^+_4Br_6]^{2-}$ layers which alternate with $[Pb_5(SeO_3)_4]^{2+}$ layers. $Pb_8Cu^{2+}(SeO_3)_4Br_{10}$ contains positively charged unique $[Pb_8Cu^{2+}(SeO_3)_4]^{10+}$ rod-like chains with Cu^{2+} cations in the core. These chains are held together by Br^- anions. $Pb_5Cu^+_4(SeO_3)_4Br_6$ and $Pb_8Cu^{2+}(SeO_3)_4Br_{10}$ belong to new structure types. $Pb_5Cu^{2+}(SeO_3)_4(Br,Cl)_4$ is a synthetic analogue of the mineral sarrabusite, $Pb_5Cu(SeO_3)_4Cl_4$, previously known from an electron diffraction study. The investigation of this synthetic equivalent of sarrabusite by conventional single-crystal X-ray diffraction provides a distinctly improved insight in this crystal structure. Cu atom has well-defined [2O+(2O+2*X*)] (*X* = halogen) distorted octahedral coordination. PbO_n and SeO_3 polyhedra interconnect via common oxygen atoms into $[Pb_5(SeO_3)_4]^{2+}$ layers parallel to (001). Cu^{2+} cations interconnect the layers into the framework with the large cavities filled by halide *X* anions. In all three new compounds described, a common feature is the formation of the selenophile substructure which is terminated by a 'lone-pair' shell that faces bromide complexes thus forming the surface of a halophile substructure.

Keywords Copper · Lead · Selenite · Bromide · Sarrabusite · Chemical vapor transport

Introduction

Copper-lead selenite bromides, until recently remained a poorly structurally characterized class of compounds. The method of chemical vapor transport (CVT) in sealed quartz ampoules significantly expanded this family several years ago (Siidra et al. 2018). Nine new compounds were described, most of which represented new structure types. Several copper-lead selenite chloride minerals are known from the fumaroles of Tolbachik volcano: prewittite, $KPb_{1.5}Cu_6Zn(SeO_3)_2O_2Cl_{10}$ (Shuvalov et al. 2013) and allochalcoselite, $Cu^+Cu^{2+}_5PbO_2(SeO_3)_2Cl_5$ (Krivovichev et al. 2006). Sarrabusite, $Pb_5Cu(SeO_3)_4Cl_4$ was described from an oxidation zone of the lead and arsenic mine at Baccu Locci, Sardinia, Italy (Campostrini et al. 1999). Selenite-bromides of lead and copper are not known in nature. In terrestrial rocks, Br minerals are extremely rare with only nine minerals known where Br is a species-defining component (Karpenko et al. 2023). However, several bromides have recently been described from volcanic fumaroles (demicheleite-Br, BiSBr: Demartin et al. 2008) and natural coal fires (ermakovite, $(NH_4)(As_2O_3)_2Br$: Karpenko et al. 2023).

The interest of the detailed study of copper selenites stems from the intriguing magnetic properties found for a

Editorial handling: G. Giester.

✉ Oleg I. Siidra
o.siidra@spbu.ru

[1] Department of Crystallography, Institute of Earth Sciences, St. Petersburg State University, University emb. 7/9, 199034 St. Petersburg, Russia

[2] Kola Science Center, Russian Acad. Sci, Murmansk Region, Fersmana str. 14, Apatity 184209, Russia

number of representatives of this family (e.g. Zhang et al. 2010; Berdonosov et al. 2018; Badrtdinov et al. 2018). However, obtaining the single-phase polycrystalline samples of complex copper selenites remains a challenge.

Prof. Dr. Josef Zemann and his group at the University of Vienna made an outstanding contribution to the crystal chemistry of copper oxides and oxysalts, including selenites and especially tellurites. A large number of his works were devoted to the crystal chemistry of compounds with 'lone-pair' cations and features of their structural architectures. Three new copper-lead selenite bromides synthesized by the CVT method, and described herein in the special issue dedicated to Josef Zemann, further contribute to this field. In one of the compounds, a new type of Cu(II) mixed-ligand coordination was revealed. All three new compounds demonstrate the use of 'lone-pair' cations as 'chemical scissors' and the segregation of the structure into regions with different types of chemical bonding.

Experimental

Synthesis

Syntheses were performed according to the protocols published in Siidra et al. (2018). The starting materials used in this study were $PbSeO_3$, CuBr, $CuBr_2$ and $CuCl_2$ (all from Vekton, analytical or extra pure grade, purity ≥ 99.5%). For the synthesis of $Pb_5Cu^+_4(SeO_3)_4Br_6$, $PbSeO_3$ and CuBr were mixed in a 1:1 molar ratio and thoroughly ground and placed in thin-walled silica ampoules (inner diameter 5 mm, length 150 mm), sealed under vacuum, and placed in a furnace. The furnace was heated to and held at 400 °C for two weeks, after which it was switched off to reach an ambient temperature. The temperature gradient between the hot and cold ends of the tube was ~ 50 °C. The two other new compounds were synthesized similarly. For the synthesis of $Pb_8Cu^{2+}(SeO_3)_4Br_{10}$, a ratio of $PbSeO_3$:$CuBr_2$ 2:1 was used,

Table 1 Crystallographic data and refinement parameters for $Pb_5Cu^+_4(SeO_3)_4Br_6$, $Pb_8Cu^{2+}(SeO_3)_4Br_{10}$ and $Pb_5Cu^{2+}(SeO_3)_4(Br,Cl)_4$

	$Pb_5Cu^+_4(SeO_3)_4Br_6$	$Pb_8Cu^{2+}(SeO_3)_4Br_{10}$	$Pb_5Cu^{2+}(SeO_3)_4(Br,Cl)_4$
Crystal data:			
Crystal system	monoclinic	orthorhombic	monoclinic
Space group	*C*2/*m*	*I*222	*C*2/*c*
Unit cell dimensions	17.7248(14)	9.5893(5)	24.590(6)
a (Å)	5.5484(5)	12.4484(9)	5.5786(14)
b (Å)	12.7010(10)	12.7927(6)	14.248(4)
c (Å)			
β (°)	103.398(2)		102.883(7)
Unit-cell volume (Å^3)	1215.08(17)	1527.08(15)	1905.3(9)
Calculated density (g·cm^{-3})	6.225	6.585	6.435
Absorption coefficient (mm^{-1})	53.83	62.50	57.64
Crystal size (mm^3)	0.06×0.06×0.04	0.10×0.10×0.14	0.20×0.16×0.10
Data collection:			
Temperature (K)	296(2)	296(2)	296(2)
Radiation, wavelength (Å)	Mo*K*α, 0.71073	Mo*K*α, 0.71073	Mo*K*α, 0.71073
F(000)	1936	2534	3113
θ range (°)	2.36 - 28.00	2.283 - 28.00	1.70 - 28.00
h, *k*, *l* ranges	-23→22 -6→7 -16→16	-12→12 -16→16 -16→16	-28→32 -7→7 -11→18
Total reflections collected	3911	7859	9259
Unique reflections (R_{int})	1567 (0.037)	1853 (0.044)	2309 (0.034)
Unique reflections $F > 4\sigma(F)$	1448	1808	1976
Structure refinement:			
Refinement method	Full-matrix least-squares on F^2		
Data/restraints/parameters	1567/0/105	1853/0/78	1853/0/78
R_1 [$F > 4\sigma(F)$], wR_2 [$F > 4\sigma(F)$]	0.024, 0.055	0.027, 0.065	0.026, 0.063
R_2 all, wR_2 all	0.028, 0.056	0.028, 0.066	0.034, 0.066
G.o.f. on F^2	1.079	1.078	1.074
CCDC*	2224683	2224684	2224686

G.o.f = goodness of fit

CCDC Cambridge Crystallographic Data Centre structure number

Table 2 Selected interatomic distances (in Å) in crystal structures of $Pb_5Cu^+_4(SeO_3)_4Br_6$ and $Pb_8Cu^{2+}(SeO_3)_4Br_{10}$

$Pb_5Cu^+_4(SeO_3)_4Br_6$				$Pb_8Cu^{2+}(SeO_3)_4Br_{10}$			
Pb1-O4	2.481(4) ×2	Cu2A…Cu2B	0.32(3)	Pb1-O2	2.422(10) ×2	Cu-O1	1.990(9) ×4
Pb1-O2	2.532(5) ×2	Cu2A-Br1	2.416(11)	Pb1-Br1	3.1001(15) ×2	Cu-O2	2.967(11) ×4
Pb1-Br2	3.3023(6) ×2	Cu2A-Br2	2.498(9)	Pb1-Br3	3.2906(16) ×2		
Pb1-Br3	3.3954(10)	Cu2A-Br3	2.505(12)	Pb1-Br3	3.4631(16) ×2	Se-O2	1.702(11)
Pb1-Br1	3.4085(11)	Cu2A-Br2	2.652(11)			Se-O1	1.720(9)
		Cu2B-Br3	2.401(15)	Pb2-O3	2.562(10)	Se-O3	1.723(10)
Pb2-O1	2.433(7)	Cu2B-Br2	2.458(14)	Pb2-O2	2.573(11)	Se-Br1	3.2264(19)
Pb2-O2	2.663(4) ×2	Cu2B-Br1	2.479(18)	Pb2-O3	2.608(10)	Se-Br1	3.3730(18)
Pb2-O4	2.710(4) ×2	Cu2B-Br2	2.751(16)	Pb2-O3	2.641(10)	Se-Br3	3.449(2)
Pb2-O4	2.721(4) ×2			Pb2-O1	2.730(9)		
Pb2-O3	2.897(2) ×2	Se1-O1	1.656(7)	Pb2-Br3	3.2830(17)		
		Se1-O2	1.717(5) ×2	Pb2-Br1	3.3442(15)		
Pb3-O3	2.557(6) ×2	Se1-Br2	3.5199(12)	Pb2-Br2	3.3537(16)		
Pb3-O2	2.666(5) ×4	Se1-Br3	3.6063(8) ×2	Pb2-Br1	3.4172(15)		
Pb3-O1	3.212(4) ×4						
		Se2-O3	1.699(7)	Pb3-O1	2.890(10) ×2		
Cu1A…Cu1B	0.390(12)	Se2-O4	1.707(5) ×2	Pb3-Br3	3.0231(14) ×2		
Cu1A-Br3	2.414(6) ×2	Se2-Br2	3.6493(13)	Pb3-Br2	3.0951(14) ×2		
Cu1A-Br1	2.615(7) ×2	Se2-Br1	3.7477(9) ×2	Pb3-Br1	3.1587(14) ×2		
Cu1B-Br1	2.322(7)						
Cu1B-Br1	2.623(5)						
Cu1B-Br3	2.414(6)						
Cu1B-Br3	2.731(7)						

and for the synthesis of $Pb_5Cu^{2+}(SeO_3)_4(Br,Cl)_4$, a ratio of $PbSeO_3$, $CuBr_2$ and $CuCl_2$ 2:1:1.

The new compounds were found in the cold zones of the tubes. Crystals of $Pb_5Cu^+_4(SeO_3)_4Br_6$ are light-brown, whereas crystals of $Pb_8Cu^{2+}(SeO_3)_4Br_{10}$ and $Pb_5Cu^{2+}(SeO_3)_4(Br,Cl)_4$ are green. Many other differently coloured crystals, including those reported in Siidra et al. (2018), were found in the different zones of the tubes. Most of them were grown in overlapping areas and in close proximity to each other; neither their colour nor their habit made it possible to distinguish clearly between the different species. Because of this, studies other than crystallographic ones have not been possible yet. Qualitative scanning electron microscope (Hitachi TM300) chemical analysis did not reveal any other elements with an atomic number greater than 11 (Na) in all studied compounds, except Cu, Br, Se, Pb, and Cl [in $Pb_5Cu^{2+}(SeO_3)_4(Br,Cl)_4$ only].

Single-crystal X-ray studies

Single crystals of all compounds were selected under the microscope and mounted on thin glass fibers for X-ray diffraction analysis using Bruker APEX II DUO X-ray diffractometer with a micro-focus X-ray tube operated with MoKα radiation at 50 kV and 0.6 mA. The data were integrated and corrected for absorption using a multi scan type model using the Bruker programs *APEX* and *SADABS*. More than a hemisphere of X-ray diffraction data was collected for each crystal. The structure refinements were performed using SHELXL software. Occupancies of partially occupied Cu sites in $Pb_5Cu^+_4(SeO_3)_4Br_6$ were first refined and later fixed in the final stages of the crystal structure refinement constrained to keep the electroneutrality of the formula. Crystallographic information for the new compounds is summarized in Table 1. Selected interatomic distances are given in Table 2, 3 and atomic coordinates, displacement parameters and valence-sums are provided in Tables 4-6.

Bond-valence analysis was done using bond-valence parameters taken from Gagné and Hawthorne (2015) for the Pb^{2+}-O, Se^{4+}-O, and Cu^{2+}-O bonds, from Brese and O'Keeffe (1991) for the Cu^{2+}-Cl, Cu^{2+}-Br, Pb^{2+}-Cl, Se^{4+}-Cl, and Se^{4+}-Br bonds and from Hu (2007) for the Pb^{2+}-Br bonds. Bond valences were not calculated for Cu^+-Br bonds in the crystal structure of $Pb_5Cu^+_4(SeO_3)_4Br_6$ due to the disorder of Cu^+ cations. All of the Pb-O and Pb-*X* bonds ≤ 3.55 Å, Se-O bonds ≤ 2.00 Å, Se-*X* bonds ≤ 3.75 Å, Cu^{2+}-O and Cu^{2+}-*X* ≤ 3.00 Å were taken into account.

Table 3 Selected interatomic distances (in Å) in crystal structures of $Pb_5Cu^{2+}(SeO_3)_4(Br,Cl)_4$ and sarrabusite, $Pb_5Cu(SeO_3)_4Cl_4$

	$Pb_5Cu^{2+}(SeO_3)_4(Br,Cl)_4$ present study	Sarrabusite $Pb_5Cu(SeO_3)_4Cl_4$ (Gemmi et al. 2012) Manual refined model	Sarrabusite $Pb_5Cu(SeO_3)_4Cl_4$ (Gemmi et al. 2012) Automated refined model		$Pb_5Cu^{2+}(SeO_3)_4(Br,Cl)_4$ present study	Sarrabusite $Pb_5Cu(SeO_3)_4Cl_4$ (Gemmi et al. 2012) Manual refined model	Sarrabusite $Pb_5Cu(SeO_3)_4Cl_4$ (Gemmi et al. 2012) Automated refined model
Pb1-O2	2.413(6)	2.47(5)	2.50(3)	Cu-O5	1.952(5) ×2	2.16(4)	2.03(3)
Pb1-O6	2.441(6)	2.32(4)	2.38(3)	Cu-O4	2.370(6) ×2	2.17(5)	2.17(3)
Pb1-O4	2.635(6)	2.96(4)	2.89(3)	Cu-*X*2	2.4376(17) ×2	2.94(3)	2.48(2)
Pb1-O3	2.732(6)	2.54(3)	2.54(3)				
Pb1-O1	2.733(6)	2.77(4)	2.79(3)	Se1-O6	1.686(5)	1.69(4)	1.74(3)
Pb1-O5	2.891(6)	2.67(4)	2.85(3)	Se1-O1	1.706(6)	1.61(5)	1.68(3)
Pb1-*X*2	3.2424(17)	3.16(3)	3.122(19)	Se1-O3	1.741(6)	1.74(4)	1.80(3)
Pb1-*X*1	3.5321(12)	3.36(4)	3.42(3)	Se1-*X*1	3.4818(15)	-	-
				Se1-*X*2	3.6323(19)	-	-
Pb2-O3	2.405(6)	2.48(4)	2.45(3)				
Pb2-O3	2.662(6)	3.04(5)	2.75(3)	Se2-O2	1.681(6)	1.70(6)	1.82(3)
Pb2-O1	2.686(6)	2.48(4)	2.45(3)	Se2-O4	1.709(6)	1.75(4)	1.71(3)
Pb2-O1	2.766(6)	3.04(5)	2.75(3)	Se2-O5	1.735(5)	1.89(4)	1.88(3)
Pb2-*X*1	3.1396(12)	2.91(3)	2.980(17)	Se2-*X*2	3.2992(18)	-	-
Pb2-*X*1	3.1591(12)	3.21(4)	3.14(2)	Se2-*X*2	3.5361(18)	-	-
Pb2-*X*2	3.1961(18)	2.82(3)	3.27(2)				
Pb2-*X*1	3.2280(12)	3.14(3)	3.134(17)				
Pb3-O6	2.526(5) ×2	2.67(4)	2.52(3)				
Pb3-O4	2.532(6) ×2	2.48(5)	2.49(3)				
Pb3-O5	2.652(6) ×2	2.69(5)	2.69(3)				
Pb3-O2	2.690(6) ×2	2.62(4)	2.52(3)				

$X1 = Br_{0.823(8)}Cl_{0.177(8)}$; $X2 = Br_{0.281(7)}Cl_{0.719(7)}$

Results and discussion: crystal structures

$Pb_5Cu^{+}_4(SeO_3)_4Br_6$

The crystal structure of $Pb_5Cu^{+}_4(SeO_3)_4Br_6$ contains three symmetrically unique Pb and two Se sites. In order to determine the coordination of Pb^{2+} cations, all bonds below 3.5 Å were taken into account. An environment of the Pb^{2+} cation is variable (Fig. 1, Table 2). Pb1 atom is coordinated by the four O and four Br atoms thus forming a distorted PbO_4Br_4 square antiprism. This type of coordination is typical for Pb^{2+} cations in Pb oxyhalides and is usually explained in terms of stereoactive behaviour of the $6s^2$ lone electron pair. Pb2 and Pb3 atoms are coordinated exclusively by oxygen atoms. The Pb2 is coordinated by nine O atoms in a modestly one-sided fashion. The Pb3 atom forms PbO_{10} irregular polyhedron.

Each of two symmetrically independent Se^{4+} cations forms three nearly equal Se^{4+}-O bonds (Table 2) in the range 1.656(7) – 1.717(5) Å. This one-sided pyramidal configuration is typical for $Se(IV)O_3$ groups.

Two Cu sites were refined each as a split atom model, thus being disordered over several neighbouring positions with very short Cu··Cu distances and low occupancies indicated in Table 4. The Cu^+ cations are located in Cu1 and Cu2 sites. Each environment can be described as a distorted Cu^+Br_4 tetrahedron, the individual values of the Cu^+-Br distances are somewhat longer compared to those in CuBr (<Cu^+-Br> = 2.46Å) (Vegard and Skofteland 1942) due to the disorder. The latter is a typical feature of Cu^+ ion in oxyhalides obtained by the CVT.

The new compound $Pb_5Cu^{+}_4(SeO_3)_4Br_6$ belongs to a new structure type. The crystal structure consists of two distinct parts: corner- and edge-sharing $CuBr_4$ tetrahedra that form unique infinite $[Cu^{+}_4Br_6]^{2-}$ layers and $[Pb(SeO_3)_4]^{2+}$ cationic layers (Fig. 1a,b). $[Cu^{+}_4Br_6]^{2-}$ layers have a topology of [PbO] layers in litharge (α-PbO). The anionic and cationic layers, are separated one from each other by an interface

Table 4 Atomic coordinates, displacement parameters (Å^2) and bond-valence sums (*B.V.S.*; in valence units, *vu*) in $Pb_5Cu^+_4(SeO_3)_4Br_6$

Atom	*B.V.S.*	*x/a*	*y/b*	*z/c*	U_{eq}	U_{11}	U_{22}	U_{33}	U_{23}	U_{13}	U_{12}
Pb1	1.98	0.20736(2)	0	0.24894(3)	0.01785(11)	0.02264(19)	0.0159(2)	0.01605(17)	0	0.00672(13)	0
Pb2	2.02	0.16141(2)	½	-0.00600(3)	0.01814(11)	0.01362(17)	0.0240(2)	0.01667(17)	0	0.00321(12)	0
Pb3	1.84	½	½	0	0.02900(15)	0.0163(3)	0.0468(4)	0.0229(3)	0	0.00256(19)	0
Br1	n/a	0.39943(6)	0	0.37459(8)	0.0276(2)	0.0227(5)	0.0316(7)	0.0267(5)	0	0.0020(4)	0
Br2	n/a	0.23400(6)	-½	0.39389(7)	0.0216(2)	0.0264(5)	0.0186(5)	0.0187(4)	0	0.0028(3)	0
Br3	n/a	0.05759(6)	0	0.37408(8)	0.0263(2)	0.0283(5)	0.0276(6)	0.0259(5)	0	0.0123(4)	0
Se1	4.08	0.05965(5)	-½	0.19334(6)	0.01231(18)	0.0127(4)	0.0141(5)	0.0102(3)	0	0.0027(3)	0
Se2	3.95	0.33617(5)	½	0.17530(6)	0.01321(19)	0.0131(4)	0.0121(5)	0.0135(4)	0	0.0011(3)	0
Cu1A[a]	n/a	½	0.281(2)	½	0.051(3)						
Cu1B[b]	n/a	0.4845(3)	0.2322(12)	0.5011(5)	0.050*						
Cu2A[c]	n/a	0.3480(6)	-0.227(2)	0.5045(7)	0.054(3)	0.064(4)	0.063(6)	0.043(3)	0.011(3)	0.028(3)	0.015(4)
Cu2B[d]	n/a	0.1512(7)	0.220(4)	0.5061(11)	0.065(4)	0.047(6)	0.069(9)	0.060(6)	-0.024(5)	-0.026(4)	0.029(5)
O1	2.13	-0.0283(4)	-0.500000	0.1124(6)	0.065(4)	0.012(4)	0.147(12)	0.031(4)	0	-0.005(3)	0
O2	1.81	0.1020(3)	-0.2667(9)	0.1393(3)	0.0213(10)	0.035(3)	0.009(2)	0.022(2)	0.0004(19)	0.0109(19)	0.000(2)
O3	2.10	0.3732(4)	0.500000	0.0633(6)	0.0295(17)	0.024(4)	0.034(5)	0.037(4)	0	0.020(3)	0
O4	1.95	0.2733(2)	0.2647(9)	0.1408(3)	0.0172(9)	0.020(2)	0.013(3)	0.019(2)	-0.0007(18)	0.0057(17)	-0.0048(19)

[a]site occupancy factor (s.o.f.) = 0.24

[b]site occupancy factor (s.o.f.) = 0.27

[c]site occupancy factor (s.o.f.) = 0.36

[d]site occupancy factor (s.o.f.) = 0.25

* - fixed during the refinement

composed of the lone pairs associated with both Se(IV) and Pb(II). The lone pairs act as chemical scissors for the lead selenite blocks by creating nonbonding interleafs separating them from anionic copper-bromide units. Similar examples of the segregation of structural parts of different kinds of chemical interaction have been previously reported in several lone-pair oxyhalide systems (Becker et al. 2003; Mayerová et al. 2006).

$Pb_8Cu^{2+}(SeO_3)_4Br_{10}$

There are three sites occupied by Pb atoms (Table 5) in the crystal structure of $Pb_8Cu^{2+}(SeO_3)_4Br_{10}$. The coordination of the Pb1 atom is asymmetric with two strong Pb1-O2 bonds located in one side of the hemisphere and six Pb1-Br bonds distributed uniformly over the coordination sphere (Fig. 2). Pb3 atom has the same CN (coordination number) and similar geometry of coordination environments, whereas Pb2 atom has a typical for Pb^{2+} cation coordination with five relatively short and strong Pb2-O bonds located in one coordination hemisphere and four long and weak Pb2-Br bonds in the other.

The crystal structure of $Pb_8Cu^{2+}(SeO_3)_4Br_{10}$ contains one symmetrically independent Cu atom (Fig. 2). All Cu^{2+}-O bonds ≤3.0 Å were taken into consideration. Cu1 atom forms four very strong Cu-O_{eq} bonds (≤ 2 Å) resulting in

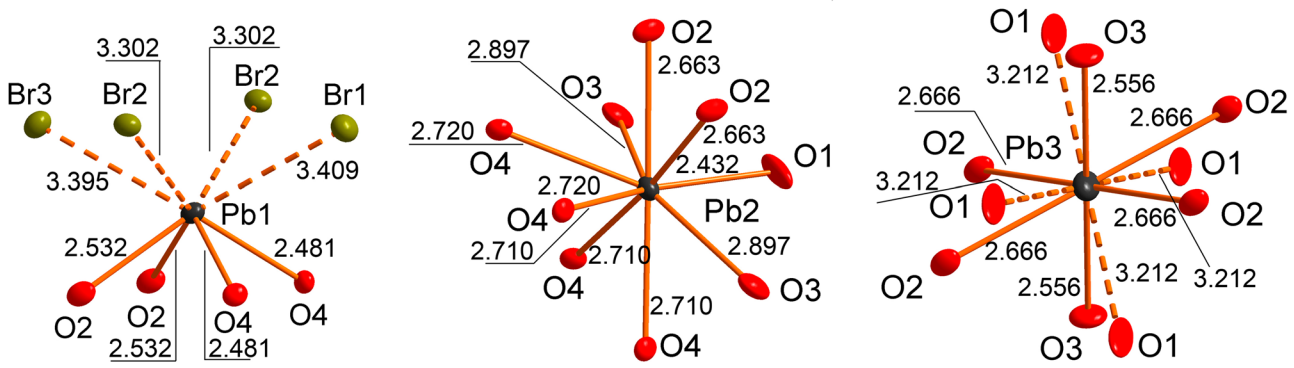

Fig. 1 Coordination of Pb^{2+} cations in the crystal structure of $Pb_5Cu^+_4(SeO_3)_4Br_6$. Displacement ellipsoids are drawn at the 50 % probability level. Long and weak Pb-Br and Pb-O bonds are shown by the dashed lines

Table 5 Atomic coordinates, displacement parameters (Å^2) and bond-valence sums (in valence units, *vu*) in $Pb_8Cu^{2+}(SeO_3)_4Br_{10}$

Atom	*B.V.S.*	*x/a*	*y/b*	*z/c*	U_{eq}	U_{11}	U_{22}	U_{33}	U_{23}	U_{13}	U_{12}
Pb1	1.98	½	0.83257(5)	0	0.01835(17)	0.0219(3)	0.0123(3)	0.0208(4)	0	0.0025(3)	0
Pb2	1.94	0.35743(5)	0.87374(4)	0.38065(4)	0.01907(15)	0.0226(2)	0.0205(2)	0.0141(3)	-0.0033(2)	0.0016(2)	-0.0008(2)
Pb3	2.05	½	½	0.31521(7)	0.02170(18)	0.0185(3)	0.0189(3)	0.0277(4)	0	0	0.0023(3)
Se1	4.01	0.26743(12)	0.63118(10)	0.12424(10)	0.0111(2)	0.0118(5)	0.0129(5)	0.0085(6)	-0.0019(5)	0.0008(4)	-0.0001(4)
Cu1	1.84	½	½	0	0.0097(5)	0.0110(11)	0.014(1)	0.0039(13)	0	0	0
Br1	1.02	0.55355(15)	0.72899(10)	0.21669(11)	0.0169(3)	0.0239(6)	0.0151(6)	0.0117(6)	-0.0020(4)	-0.0015(5)	-0.0010(5)
Br2	0.73	½	0.66049(15)	½	0.0235(4)	0.0420(10)	0.0150(8)	0.0134(9)	0	0.0054(10)	0
Br3	0.89	0.68809(14)	0.98878(14)	0.84773(12)	0.0225(3)	0.0187(6)	0.0316(8)	0.0171(7)	0.0015(6)	0.0033(5)	0.0000(6)
O1	2.02	0.3614(9)	0.5139(7)	0.1150(8)	0.0142(17)	0.016(4)	0.016(4)	0.011(4)	-0.002(4)	0.002(4)	0.003(4)
O2	2.02	0.3227(11)	0.6948(8)	0.0140(9)	0.020(2)	0.023(4)	0.022(5)	0.016(6)	0.006(4)	-0.003(4)	-0.009(4)
O3	2.05	0.1120(10)	0.5803(8)	0.0782(8)	0.0140(19)						

a CuO_4 square which is complemented by four very long Cu-O_{ap} bonds of 2.967(11) Å each. These four Cu1-O2 bonds contribute 0.12 *v.u.* to the bond-valence sum of Cu1. Taking Cu1-O2 bonds into account, the overall coordination polyhedron of Cu^{2+} can be considered as "an octahedron with two split vertices". A similar [4+4] coordination mode was observed in several copper phosphates (Anderson et al. 1981; Escobal et al. 2006; Senga and Kawahara 1980; Yakubovich et al. 2008). Cu^{2+} coordination environments with CN >6 in minerals and synthetic compounds with TO_4 anions were recently reviewed in Siidra et al. (2021).

There is one symmetrically independent selenium site in the crystal structure of $Pb_8Cu^{2+}(SeO_3)_4Br_{10}$. The Se^{4+} cation has a typical oxygen coordination of triangular pyramid.

Due to the variability of Pb^{2+} coordination, it is necessary to determine strongly bonded structural units in terms of bond-valence considerations. The selenite groups are isolated from each other and linked through Pb-O bonds. The crystal structure of $Pb_8Cu^{2+}(SeO_3)_4Br_{10}$ exhibits a 1*D* structure, consisting of positively charged unique $[Pb_8Cu^{2+}(SeO_3)_4]^{10+}$ rod-like chains (Figs. 3a, 4) with Cu^{2+} cations in the core. The chains extend along the *a* axis and they are mutually held together by the Br^- anions.

$Pb_5Cu^{2+}(SeO_3)_4(Br,Cl)_4$

The chemical formula and general crystallographic data of the new compound $Pb_5Cu^{2+}(SeO_3)_4(Br,Cl)_4$ are similar

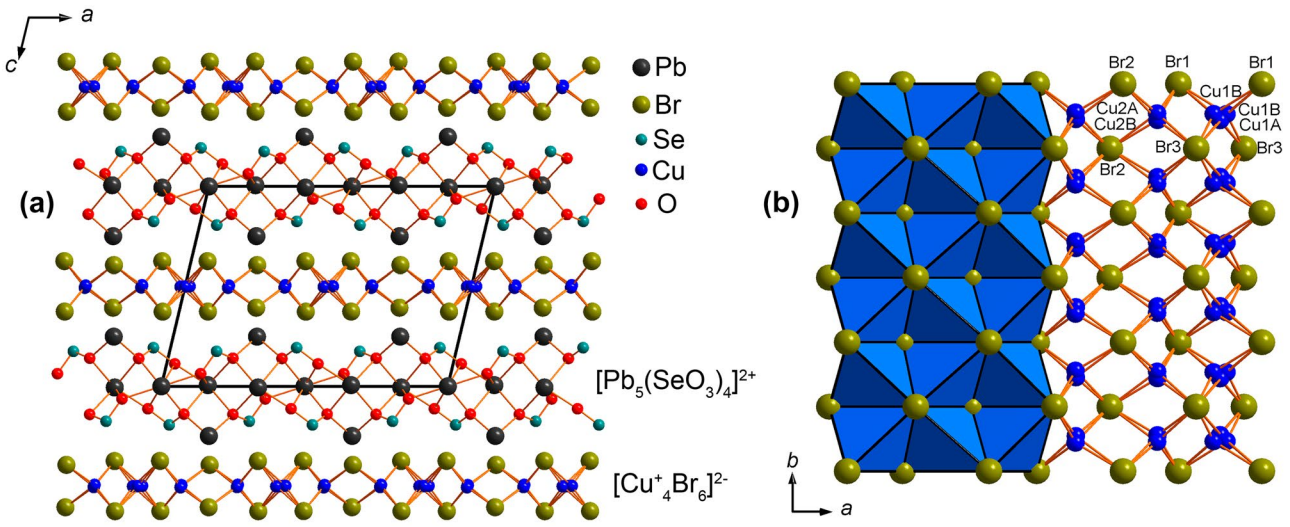

Fig. 2 General projection of the crystal structure of $Pb_5Cu^+_4(SeO_3)_4Br_6$ (**a**). $[Cu^+_4Br_6]^{2-}$ tetrahedral layer in the structure of $Pb_5Cu^+_4(SeO_3)_4Br_6$ in balls-and-sticks and polyhedral representation (Cu^+Br_4 tetrahedra are shown in blue) (**b**)

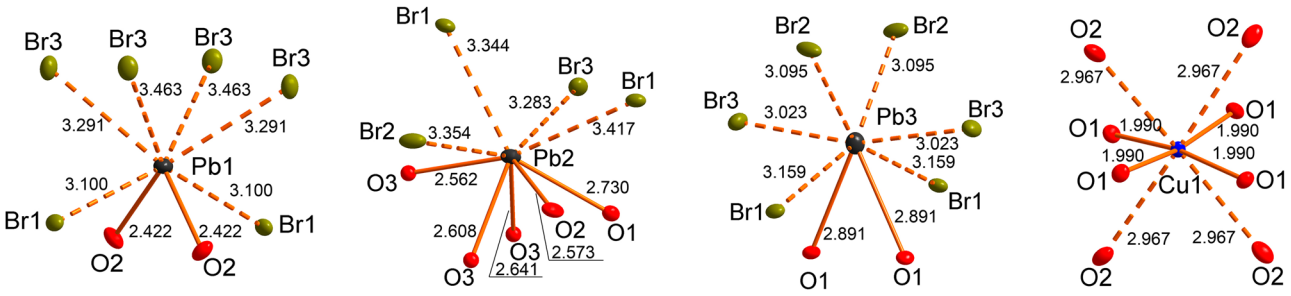

Fig. 3 Coordination of Pb^{2+} and Cu^{2+} cations in the crystal structure of $Pb_8Cu^{2+}(SeO_3)_4Br_{10}$. Displacement ellipsoids are drawn at the 50 % probability level. Pb-Br bonds and long Cu1-O2 bonds are shown by the dashed lines

to the mineral sarrabusite $Pb_5Cu(SeO_3)_4Cl_4$ (Gemmi et al. 2012). The crystal structure of sarrabusite has been determined using an electron diffraction tomography technique. Some of the reported cation-anion distances calculated on the basis of the refined models (manual or automated) show significant differences depending on the model (Table 3). Therefore, the determination of the structure of the synthetic sarrabusite by conventional single-crystal X-ray diffraction is important for clarifying the coordination of cations and revealing features of the crystal structure. The coordinates from Gemmi et al. (2012) were taken as a starting model for the structure refinement.

The crystal structure of the synthetic $Pb_5Cu^{2+}(SeO_3)_4(Br,Cl)_4$ contains three symmetrically independent Pb sites occupied by Pb atoms, one Cu site occupied by Cu atoms and two Se sites (Table 6). The crystal structure also contains two *X* halide sites. *X*1 site is predominantly occupied by bromine ($Br_{0.823(8)}Cl_{0.177(8)}$), whereas position *X*2 is predominantly occupied by chlorine ($Br_{0.281(7)}Cl_{0.719(7)}$).

The two independent SeO_3 groups show the usual triangular pyramidal shape with Se-O bond lengths varying from 1.681(6) to 1.741(6) Å depending on their bonding to Pb and Cu. No significant elongations of the Se-O bonds like Se2-O5 = 1.89(4) Å (Table 3) reported by Gemmi et al. (2012) were found in the crystal structure of the synthetic $Pb_5Cu^{2+}(SeO_3)_4(Br,Cl)_4$.

Pb1 atom has mixed ligand coordination by six oxygen anions in the range 2.413(6)-2.891(6) Å and two *X* anions at much longer distances 3.2424(17)-3.5321(12) Å. The Pb2 site is coordinated by four O and four *X* atoms (Fig. 5). The resulting PbO_4X_4 polyhedron is a square antiprism very similar in geometry to Pb1 atom in $Pb_5Cu^{+}{}_4(SeO_3)_4Br_6$ and to the mixed ligand coordination of Pb^{2+} cations in Pb oxyhalides in general. Pb3 atom is coordinated by eight oxygen atoms thus forming relatively symmetrical coordination environments similar to Pb2 atom in $Pb_5Cu^{+}{}_4(SeO_3)_4Br_6$ described above.

Cu^{2+} cation coordination is well-defined in $Pb_5Cu^{2+}(SeO_3)_4(Br,Cl)_4$ and differs notably from the Cu [4O+2Cl] coordination reported by Gemmi et al. (2012). All Cu-O and Cu-*X* bonds shorter than 3.2 Å are included into the Cu coordination sphere. Cu forms two strong Cu-O bonds 1.952(5) Å each with O5 atoms (Table 3; Fig. 5). Two Cu1-O4 bonds are significantly elongated up to 2.370(6) Å each. The coordination is complemented by two Cu-*X*2 bonds of 2.4376(17) Å each. Thus, Cu has [2O+(2O+2*X*)] strongly distorted octahedral coordination. To the best of our knowledge, this type of Cu^{2+} mixed-ligand coordination has never been described in divalent copper oxyhalide synthetic compounds and minerals (Krivovichev et al. 2013). However, similar in geometry [2OH+4O] octahedral coordination by O/OH is well-known e.g. for volborthite $Cu_3V_2O_7(OH)_2{\cdot}2H_2O$ (Ginga et al. 2021). This type of coordination in volborthite was explained by Burns and Hawthorne (1996) by the dynamic Jahn-Teller effect. Note, *X*1 site predominantly occupied by Br is bonded to Pb atoms only, whereas *X*2 site mostly occupied by Cl is bonded to both Pb and Cu.

Because of the large size and variability of coordination polyhedra around Pb^{2+} cations and the strength of the Pb-O and Se-O bonds in comparison to the Pb-*X* bonds, it is convenient to describe the substructure of $Pb_5Cu^{2+}(SeO_3)_4(Br,Cl)_4$ in PbO_n and SeO_3 polyhedra. The latter interconnect via common oxygen atoms into $[Pb_5(SeO_3)_4]^{2+}$ layers parallel to (001) (Fig. 6a). Cu^{2+} cations interconnect the layers into the framework shown in Fig. 6b. The large cavities are filled by halide *X* anions.

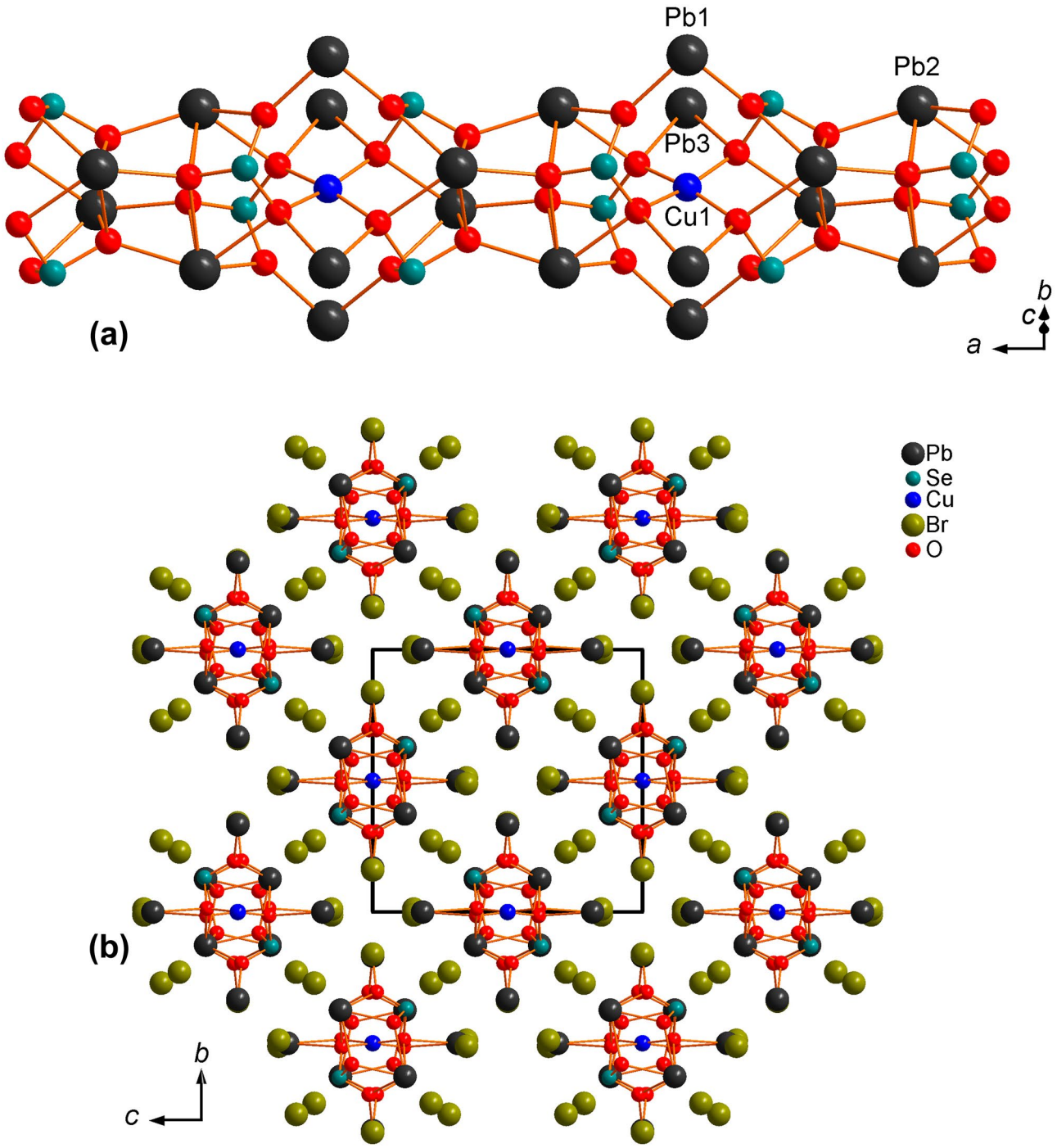

Fig. 4 $[Pb_5Cu^{+}{}_4(SeO_3)_4]^{6+}$ cationic rod-like chains in the structure of $Pb_8Cu^{2+}(SeO_3)_4Br_{10}$ (**a**). General projection of the crystal structure of $Pb_8Cu^{2+}(SeO_3)_4Br_{10}$ (**b**)

Table 6 Atomic coordinates, displacement parameters (Å^2) and bond-valence sums (in valence units, *vu*) in $Pb_5Cu^{2+}(SeO_3)_4(Br,Cl)_4$

Atom	*B.V.S.*	*x/a*	*y/b*	*z/c*	U_{eq}	U_{11}	U_{22}	U_{33}	U_{23}	U_{13}	U_{12}
Pb1	1.88	0.10398(2)	0.03948(6)	0.17919(2)	0.01721(10)	0.01567(16)	0.02082(18)	0.01594(16)	-0.00114(12)	0.00520(11)	-0.00082(12)
Pb2	1.95	0.26854(2)	-0.00104(6)	0.36598(2)	0.01843(10)	0.01670(17)	0.02071(18)	0.01799(16)	0.00148(12)	0.00409(12)	0.00436(12)
Pb3	2.24	0	0.53164(8)	¼	0.01513(11)	0.0138(2)	0.0177(2)	0.0145(2)	0.000	0.00454(15)	0.000
Se1	3.88	0.16593(3)	0.48374(13)	0.32764(6)	0.01303(17)	0.0119(4)	0.0143(4)	0.0136(4)	-0.0009(3)	0.0043(3)	-0.0009(3)
Se2	3.92	0.04406(3)	-0.01365(13)	0.41225(5)	0.01190(16)	0.0104(3)	0.0138(4)	0.0112(4)	0.0013(3)	0.0020(3)	0.0004(3)
Cu1	1.85	0	½	½	0.0135(3)	0.0137(6)	0.0144(7)	0.0131(6)	0.0042(5)	0.0046(5)	-0.0004(5)
*X*1	0.82	0.30042(4)	0.48992(16)	0.47167(7)	0.0214(4)	0.0195(5)	0.0191(6)	0.0275(6)	-0.0003(4)	0.0095(4)	-0.0008(3)
*X*2	0.77	0.10159(6)	0.5124(3)	0.53341(12)	0.0221(5)	0.0171(8)	0.0229(9)	0.0268(9)	-0.0005(6)	0.0060(6)	0.0000(6)
O1	1.90	0.1844(2)	0.7268(11)	0.2691(4)	0.0197(13)	0.016(3)	0.018(3)	0.025(3)	0.005(2)	0.005(3)	-0.003(2)
O2	2.01	0.0662(2)	0.9088(11)	0.3131(4)	0.0209(13)	0.020(3)	0.028(3)	0.021(3)	-0.001(3)	0.016(2)	-0.002(3)
O3	2.05	0.1992(2)	0.2630(11)	0.2746(4)	0.0189(13)	0.013(3)	0.022(3)	0.022(3)	-0.001(2)	0.005(2)	0.006(2)
O4	2.00	-0.0023(2)	0.2143(10)	0.3761(4)	0.0191(13)	0.013(3)	0.018(3)	0.027(3)	0.006(2)	0.006(2)	0.002(2)
O5	2.05	-0.0061(2)	0.7661(10)	0.4093(4)	0.0158(12)	0.015(3)	0.019(3)	0.013(3)	0.006(2)	0.004(2)	-0.005(2)
O6	2.08	0.1009(2)	0.4126(11)	0.2674(4)	0.0203(13)	0.007(3)	0.022(3)	0.031(3)	-0.005(3)	0.005(2)	-0.002(2)

$X1 = Br_{0.823(8)}Cl_{0.177(8)}$; $X2 = Br_{0.281(7)}Cl_{0.719(7)}$

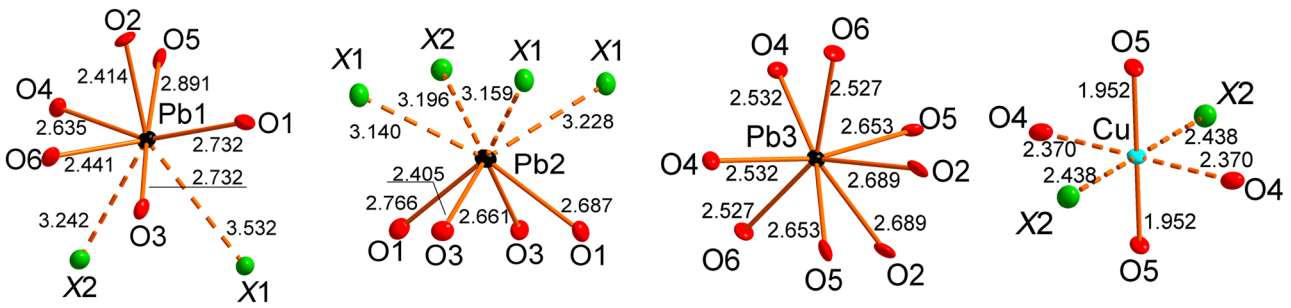

Fig. 5 Coordination of Pb^{2+} and Cu^{2+} cations in the crystal structure of $Pb_5Cu^{2+}(SeO_3)_4(Br,Cl)_4$. Displacement ellipsoids are drawn at the 50 % probability level. Pb-*X* (*X* = Br, Cl) bonds and long Cu1-*X*2, Cu1-O6 bonds are shown by the dashed lines

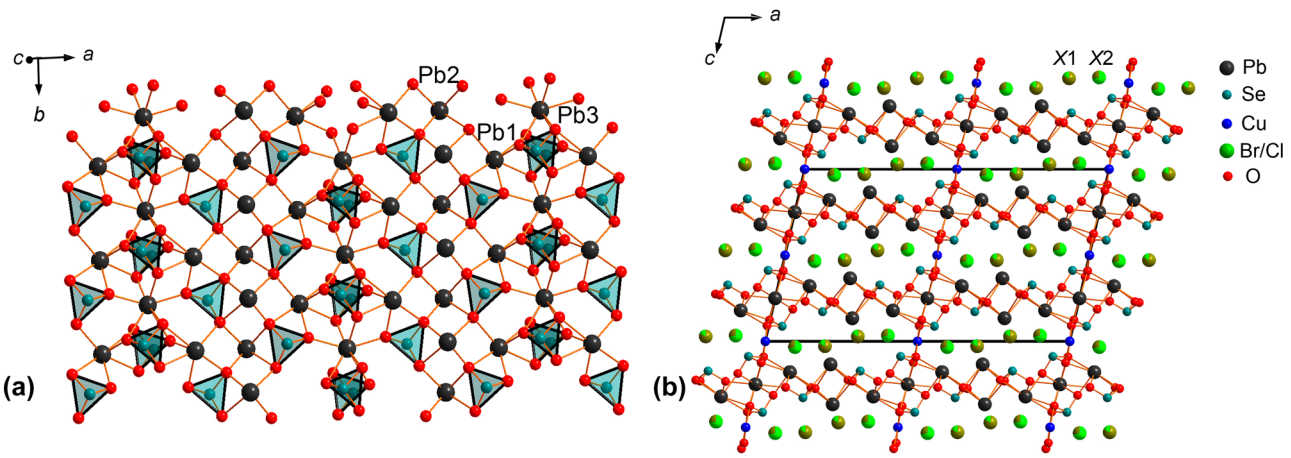

Fig. 6 $[Pb_8(SeO_3)_4]^{8+}$ layers in the structure of $Pb_5Cu^{2+}(SeO_3)_4(Br,Cl)_4$ (**a**). General projection of the crystal structure of $Pb_5Cu^{2+}(SeO_3)_4(Br,Cl)_4$ (**b**)

Concluding remarks

Our studies have revealed three new compounds in the Cu–Pb–Se–O–Br/Cl system. Chemical vapor transport is a technique which has been successfully employed for the synthesis of single crystals of copper oxysalts with intriguing magnetic properties (Han et al. 2011; Siidra et al. 2020; Ginga et al. 2022). One of the new compounds, namely $Pb_5Cu^{2+}(SeO_3)_4(Br,Cl)_4$, is isotypic with sarrabusite. Refinement of this crystal structure by the X-ray diffraction allowed to obtain a more precise picture of this compound. The synthesis of $Pb_5Cu^{2+}(SeO_3)_4(Br,Cl)_4$ by the CVT method shows the possibility of the formation of sarrabusite not only in oxidation zones (Campostrini et al. 1999) but also from the gas in volcanic fumaroles. It has not yet been possible to obtain a pure bromide analogue of sarrabusite, which may be due to the important stabilizing role of chlorine in this crystal structure. Note that chloride analogs are not known to date for the other two new compounds, as well as for the most of the compounds previously described in the Cu–Pb–Se–O–Br system in Siidra et al. (2018).

In all three new compounds described, a common feature is the formation of the selenophile substructure which is terminated by a 'lone-pair' shell that faces bromide complexes thus forming the surface of a halophile substructure. Se-Br and Se-*X* (*X*=Br, Cl) interactions also seem to be important for the stabilization of the obtained structural architectures. The Se-Br distances in the structures of new compounds vary from 3.226(2) Å in $Pb_8Cu^{2+}(SeO_3)_4Br_{10}$ to 3.7477(9) Å in $Pb_5Cu^{+}{}_4(SeO_3)_4Br_6$ (Tables 2, 3). Importance of the Se^{4+}-Cl attractive interactions has been recently analyzed by Krivovichev and Gorelova (2018). These interactions were classified into two types: interactions with the essential covalent contribution and closed-shell interactions. Apparently, similar interactions also take place in the family of selenite-bromides.

Acknowledgements Technical support by the St. Petersburg State University X-ray Diffraction Resource Centre is gratefully acknowledged. We are grateful to two anonymous reviewers and Guest Editor Gerald Giester for their many valuable comments.

References

Anderson JB, Kostiner E, Ruszala FA (1981) The crystal structure of $Ca_3Cu_3(PO_4)_4$. J. Solid State Chem. 39:29–34

Badrtdinov DI, Kuznetsova ES, Verchenko VY, Berdonosov PS, Dolgikh VA, Mazurenko V, Tsirlin AA (2018) Magnetism of coupled spin tetrahedra in ilinskite-type $KCu_5O_2(SeO_3)_2Cl_3$. Sci Rep 8:2379

Becker R, Johnsson M, Kremer R, Lemmens P (2003) Crystal structure, magnetic properties and conductivity of $CuSbTeO_3Cl_2$. Solid State Sci. 5:1411–1416

Berdonosov PS, Kuznetsova ES, Dolgikh VA (2018) Transition metal selenite halides: a fascinating family of magnetic compounds. Crystals 8:159

Brese NE, O'Keeffe M (1991) Bond-valence parameters for solids. Acta Crystallogr B47:192–197

Burns PC, Hawthorne FC (1996) Static and dynamic Jahn-Teller effects in Cu^{2+} oxysalt minerals Can Mineral 34:1089–1105

Campostrini I, Gramaccioli CM, Demartin F (1999) Orlandiite, $Pb_3Cl_4(SeO_3)_3{\bullet}H_2O$, a new mineral species, and an associated lead-copper selenite chloride from the Baccu Locci mine, Sardinia, Italy. Can Mineral 37:1493–1498

Demartin F, Gramaccioli CM, Campostrini I, Orlandi P (2008) Demicheleite, BiSBr, a new mineral from La Fossa crater, Vulcano, Aeolian Islands, Italy. Am Mineral 93:1603–1607

Escobal J, Pizarro JL, Mesa JL, Larranaga A, Fernandez JR, Arriortua MI, Rojo T (2006) Neutron diffraction, specific heat and magnetic susceptibility of $Ni_3(PO_4)_2$. J. Solid State Chem. 179:3052–3058

Gagné OC, Hawthorne FC (2015) Comprehensive derivation of bond-valence parameters for ion pairs involving oxygen. Acta Crystallogr B 71:561–578

Gemmi M, Campostrini I, Demartin F, Gorelik TE, Gramaccioli CM (2012) Structure of the new mineral sarrabusite, $Pb_5CuCl_4(SeO_3)_4$, solved by manual electron-diffraction tomography. Acta Crystallogr B 68:15–23

Ginga VA, Siidra OI, Ugolkov VL, Bubnova RS (2021) Refinement of the crystal structure and features of the thermal behavior of volborthite $Cu_3V_2O_7(OH)_2{\cdot}2H_2O$ from the Tyuya-Muyun deposit, Kyrgyzstan. Zapiski Rossiyskogo Mineralogicheskogo Obshchestva 150:115–133 ((In Russian))

Ginga VA, Siidra OI, Breitner F, Jesche A, Tsirlin AA (2022) Chemical vapor transport synthesis of $Cu(VO)_2(AsO_4)_2$ with two distinct spin-1/2 magnetic ions. Inorg. Chem. 61:16539–16548

Han TH, Helton JS, Chu S, Prodi A, Singh DK, Mazzoli C, Müller P, Nocera DG, Lee YS (2011) Synthesis and characterization of single crystals of the spin-1/2 kagome-lattice antiferromagnets $Zn_xCu_{4-x}(OH)_6Cl_2$. Phys Rev B 83:100402

Hu S-Z (2007) A new approach to bond valence parameters for Pb(II)-halide bonds. Acta Phys Chim Sin 23:786–789 ((in Chinese))

Karpenko VYu, Pautov LP, Siidra OI, Mirakov M, Zaitsev AN, Plechov PYu, Makhmadsharif S (2023) Ermakovite $(NH_4)(As_2O_3)_2Br$, a new exhalative arsenite bromide mineral from the Fan-Yagnob coal deposit, Tajikistan. Mineral Mag 87:69–78.

Krivovichev SV, Filatov SK, Burns PC, Vergasova LP (2006) The crystal structure of allochalcoselite, $Cu^{+}Cu^{2+}{}_5PbO_2(SeO_3)_2Cl_5$, a mineral with well-defined Cu^{+} and Cu^{2+} positions. Can. Mineral. 44:507–514

Krivovichev SV, Filatov SK, Vergasova LP (2013) The crystal structure of ilinskite, $NaCu_5O_2(SeO_3)_2Cl_3$, and review of mixed-ligand CuO_mCl_n coordination geometries in minerals and inorganic compounds. Miner Petrol 107:235–242

Krivovichev SV, Gorelova LA (2018) Se-Cl interactions in selenite chlorides: a theoretical study. Crystals 8:193

Mayerová Z, Johnsson M, Lidin S (2006) Lone-pair interfaces that divide inorganic materials into ionic and covalent parts. Angew Chem Int Edit 45:5602–5606

Senga Y, Kawahara A (1980) The structure of synthetic copper sodium phosphate: $Cu_9Na_6(PO_4)_8$. Acta Crystallogr B 36:2555–2558

Shuvalov RR, Vergasova LP, Semenova TF, Filatov SK, Krivovichev SV, Siidra OI, Rudashevsky NS (2013) Prewittite, $KPb_{1.5}Cu_6Zn(SeO_3)_2O_2Cl_{10}$, a new mineral from Tolbachik. Am Mineral 98:463–469

Siidra OI, Kozin MS, Depmeier W, Kayukov RA, Kovrugin VM (2018) Copper-lead selenite bromides: A new large family of compounds partly having Cu^{2+} substructures derivable from Kagome-nets. Acta Crystallogr B 74:712–724

Siidra OI, Vladimirova VA, Tsirlin AA, Chukanov NV, Ugolkov VL (2020) $Cu_9O_2(VO_4)_4Cl_2$, the first copper oxychloride vanadate: mineralogically inspired synthesis and magnetic behavior. Inorg Chem 59:2136–2143

Siidra OI, Charkin DO, Kovrugin VM, Borisov AS (2021) K(Na,K)$Na_2[Cu_2(SO_4)_4]$: a new highly porous anhydrous sulfate and evaluation of possible ion migration pathways. Acta Crystallogr B 77:1003–1011

Vegard L, Skofteland G (1942) Roentgenometrische Untersuchungen der aus den Substanzen CuCl, CuBr und CuI gebildeten binaeren Mischkristallsysteme. Archiv for Mathematik og Naturvidenskab 45:163–192

Yakubovich OV, Steele IM, Dimitrova OV (2008) A new type of mixed anionic framework in microporous rubidium copper vanadyl(V) phosphate, $Rb_2Cu(VO_2)_2(PO_4)_2$. Acta Crystallogr C 64:i62–i65

Zhang D, Berger H, Kremer RK, Wulferding D, Lemmens P, Johnsson M (2010) Synthesis, crystal structure and magnetic properties of the copper selenite chloride: $Cu_5(SeO_3)_4Cl_2$. Inorg Chem 49:9683–9688